Diamond & Related Materials 25 (2012) 134–138

Contents lists available at SciVerse ScienceDirect

Diamond & Related Materials

journal homepage: www.elsevier.com/locate/diamond

Electron field emission properties of vertically aligned carbon nanotube point emitters

Guohai Chen, S. Neupane, W.Z. Li *

Department of Physics, Florida International University, Miami, FL 33199, USA

ARTICLE INFO

Article history:
Received 30 August 2011
Received in revised form 4 March 2012
Accepted 5 March 2012
Available online 10 March 2012

Keywords:
Carbon nanotubes
Plasma enhanced chemical vapor deposition
Field emission
Point emitter
Cu wire

ABSTRACT

We fabricated vertically aligned carbon nanotube (CNT) point emitters directly on Cu wires with flat or sharp tips. The nanostructures and field emission properties of the two kinds of emitters were investigated. Both emitters showed vertically aligned, multi-walled bamboo-liked CNT structures and demonstrated good field emission properties. The emitter on the Cu wire with a flat tip (F-tip) attained an emission current of 70 μA at 4200 V whereas the emitter on the Cu wire with a sharp tip (S-tip) reached an emission current of 65 μA at 3700 V. Both of them demonstrated excellent field emission stability for 40 h at emission currents of about 40 μA and 10 μA for the F-tip and S-tip emitters, respectively.

1. Introduction

Carbon nanotubes (CNTs) are considered as the next generation cold emitters due to their high field enhancement factor, good mechanical strength, and chemical stability [1–3]. CNTs have been extensively studied for field emission applications such as field emission displays, lamps, X-ray sources, high-resolution electron-beam instruments, and microwave amplifiers [4–7]. The CNT point emitter exhibits a promising choice for some applications such as X-ray sources and electron beam sources because of the small spot size of the electron beam in comparison with the planar field emission electron sources [8]. CNT point emitters can be fabricated by direct growth [9] or by attaching CNTs on tungsten (W) wire [10] or by other methods [11]. Even though these CNT point emitters have demonstrated excellent emission characteristics, they have limited practical application due to the dramatic degradation of the emission capability during emission process. The degradation is often associated with the poor adhesion between the CNTs and the substrate or the shortening of CNTs during the emission process [12]. Few improvements have been made to resolve these issues.

Vertically aligned CNTs (VACNTs) show better field emission performance as compared to the randomly oriented CNTs [13,14]. VACNTs have been synthesized on large substrates by various methods [15–17]. In this study, VACNT point emitters were directly grown on Cu wires with a flat tip or a sharp tip using direct current (DC) plasma enhanced chemical vapor deposition (PECVD) method. The nanostructures and the field emission properties of the two kinds of VACNT point emitters were investigated. The CNT point emitters demonstrated good field emission properties, especially the excellent field emission stability at high current level. To the best of the authors' knowledge, this is the first attempt to use Cu wires as substrates to directly grow VACNTs.

2. Experiment

Cu has fully filled 3d-orbitals preventing the formation of covalent bonds with hydrocarbon molecules. Also, the small binding energy of Cu with carbon subdues the process of graphitization. Furthermore, Cu has low C solubility refraining the saturation of C atoms required to form the CNT structures [18]. To overcome these problems, a thin buffer layer of Cr has been deposited on the Cu wire prior to the deposition of a Ni catalyst layer to ensure the synthesis and good adhesion of CNTs with the Cu wire. Fig. 1 shows the schematic of the Cu wires before and after the synthesis of VACNTs. Cu wire with a diameter of 1 mm was cut into segments with a length of 5 mm using scissors. A flat tip (F-tip) was made by polishing one end of the Cu wire using a sand paper while a sharp tip (S-tip) was obtained by etching the Cu wire chemically in a 35 wt% $FeCl_3$ solution for 4 h. The F-tip and the S-tip were cleaned in acetone bath by ultrasonication, and followed by a similar treatment in alcohol bath to remove any contaminants. The sharpness of the S-tip was confirmed by an observation through the optical microscope. It is found that the sharpness of the S-tip is similar to that of a sewing needle with a tapered tip. Fig. 1a depicts the shapes of Cu F-tip and S-tip before the CNT growth. The prepared Cu wires were then coated with a Cr layer with a thickness of about 15 nm as a buffer layer and then followed by a Ni layer with a thickness of 6 nm as a catalyst film using e-beam evaporation method. VACNTs on the F-tip and S-tip were synthesized using NH_3/

* Corresponding author. Tel.: +1 305 348 7257; fax: +1 305 348 6700.
E-mail address: liwenzhi@fiu.edu (W.Z. Li).

0925-9635/$ – see front matter © 2012 Elsevier B.V. All rights reserved.
doi:10.1016/j.diamond.2012.03.002

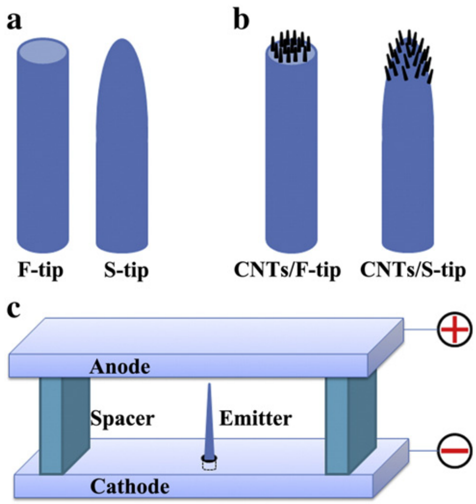

Fig. 1. A schematic of the F-tip and S-tip point emitters (a) before and (b) after CNT growth. (c) A schematic of the setup for field emission measurement.

C_2H_2 at 510 °C under a pressure of 8 Torr with a plasma power of 80 W for 10 min in a PECVD chamber. The gas flow was maintained at 100 sccm for NH_3 and 30 sccm for C_2H_2, respectively. The emitters formed by growing VACNTs on the ends of the F-tip and S-tip are illustrated in Fig. 1b, and they will be named as F-tip emitter and S-tip emitter, respectively, in the following text. Due to the shape difference between the two kinds of point emitters, the morphologies of CNTs and the consequent field emission properties might show significant difference. It is expected that the S-tip emitter can demonstrate excellent field emission performance.

The CNT morphologies of the two kinds of point emitters were characterized by scanning electron microscopy (SEM, JEOL JSSM-6330F). A transmission electron microscope (TEM, JEOL-2010F) analysis was conducted to investigate the structure and crystallinity of the CNTs. For TEM characterization, the CNTs were dispersed in alcohol by ultrasonication and then transferred onto a carbon coated TEM microgrid. Field emission measurements were carried out using a point-to-plane diode configuration in a vacuum chamber at a pressure level of 10^{-7} Torr. The measurement setup is demonstrated in Fig. 1c. The anode and cathode were stainless steel plates. The Cu wire emitter was attached firmly in a hole in the cathode by applying Ag paste. The Ag paste will also enable a good electrical contact between the cathode and the Cu wire emitter during the field emission experiments. Two ceramic plates were used as spacers. The gap between the cathode and the anode was about 500 μm. The whole setup was held rigid by tightening with screws and mounted inside a vacuum chamber to measure the field emission properties. The emission current was measured by a Keithley 4200-SCS, and DC power was provided by a DC power supply (Matsusada AU-15P20).

3. Results and discussion

The CNT morphologies of the two kinds of point emitters are shown in Fig. 2. Both of the CNTs were synthesized under identical conditions. However, the two kinds of point emitters showed quite different morphologies. The CNTs of the F-tip emitter showed a tapered shape with good vertical alignment, as shown in Fig. 2a. The length of the CNTs was about 1.5 μm. The F-tip emitter consisted of a very high density of aligned CNTs. However, the CNTs of the S-tip emitter demonstrated a quite different structure. As shown in Fig. 2b, the CNTs of the S-tip emitter showed a cylindrical stem and a coarse tip. The CNTs of the S-tip emitter had a short length in the range of 0.7–1.0 μm and showed a fairly low density as compared with that of the F-tip emitter. The low density of CNTs may result in good field emission due to the reduction of the screening effect [19]. Another obvious feature of the CNTs of the S-tip emitter is that they tend to grow connected to form bundles. The difference of morphologies between the two kinds of point emitters was probably attributed to the difference of electric field distribution during the PECVD growth due to the shape difference between the F-tip and the S-tip. The S-tip will result in higher electric field gradient around the tip. As a result, some of the Ni catalyst particles might be destroyed or etched away by the plasma. This contributes to the low density of CNTs on the S-tip as compared to the high density on the F-tip.

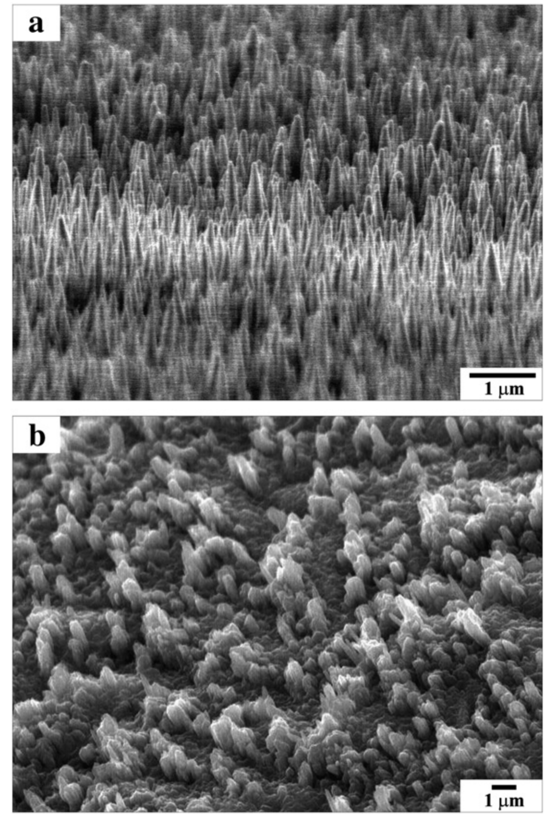

Fig. 2. SEM images of the two kinds of point emitters. (a) The F-tip emitter. (b) The S-tip emitter.

TEM observations were used to investigate the nanostructure and crystallinity of the as-synthesized CNTs. Fig. 3a shows a low magnification TEM image of the dispersed CNTs from the F-tip emitter. The CNTs displayed a multi-walled bamboo-liked structure. A catalyst particle was encapsulated inside the CNT tip, indicating the growth of the CNTs followed the tip growth model [20]. The CNT had a large diameter of 110–140 nm at the tip and around 300 nm at the stem. High resolution TEM image indicated the CNT showed well-graphitized outer walls whereas the inner walls showed a bamboo-liked structure. Some amorphous carbon materials were found on the surface of the CNTs and might be produced during the TEM sample preparation. The inset in Fig. 3a shows a high magnification TEM image of the tip of a CNT, revealing the highly ordered crystalline structures of both the carbon layers and the inside catalyst particle. TEM examination indicated that the CNT of the S-tip have a diameter of around 100 nm, as shown in Fig. 3b. However, it is very difficult to get a clear TEM image for a single CNT on the S-tip emitter because the CNTs are often connected together. Even though it is hard to know the crystallinity of the CNTs through TEM images, it is speculated that the CNTs of the S-tip emitter also had highly graphitized structures because the emitter demonstrated excellent field emission characteristics and good stability (more discussions to follow).

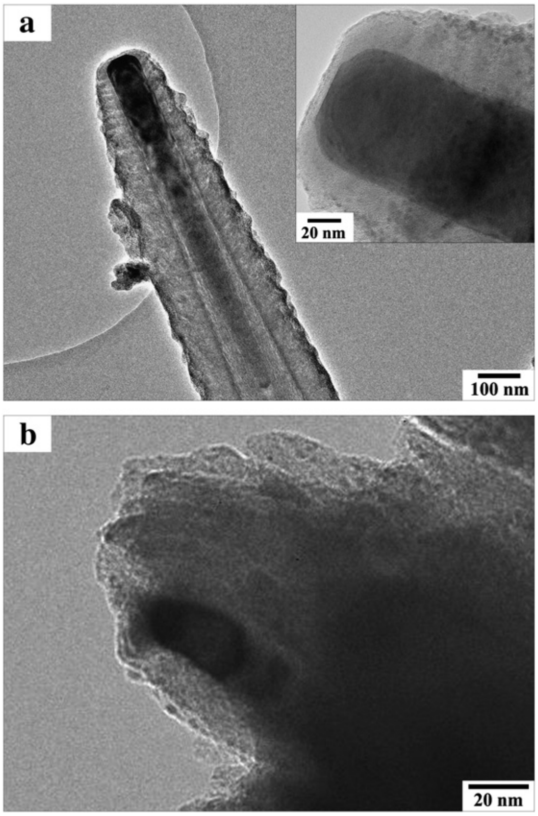

Fig. 3. TEM images of the two kinds of point emitters. (a) The F-tip emitter. (b) The S-tip emitter.

The field emission characteristics of the two kinds of CNT point emitters are shown in Fig. 4. Fig. 4a shows the current versus voltage (*I–V*) curves of the two kinds of point emitters. Both CNT point emitters demonstrated excellent field emission properties regardless of the shape of the tip of the Cu wires. We tested both the F-tip and S-tip emitters before CNT growth and could not get any emission current from either of them even when the applied voltage was increased to 5000 V. Therefore, we claimed that the excellent field emission performance was attributed to the CNTs grown on both tips. The turn-on voltage is the applied voltage to obtain an emission current of 0.1 μA. The F-tip emitter showed a turn-on voltage of about 2450 V. The S-tip emitter demonstrated a lower turn-on voltage of 2100 V compared with the F-tip emitter, indicating that the S-tip emitter had a better field emission performance than the F-tip emitter. In addition, the F-tip emitter reached the highest emission current of 70 μA at an applied voltage of 4200 V. On the contrary, the S-tip emitter obtained the highest emission current of 65 μA at 3700 V. These emission current levels are good enough for practical applications.

Fig. 4b shows the corresponding Fowler–Nordheim (F–N) plots. The straight lines indicate the quantum mechanical tunneling characteristic of the field electron emission. The field enhancement factor can be calculated using the F–N equation:

$$I = \left(A\alpha\beta^2 V^2/d^2\phi\right)\exp\left[-B\phi^{3/2} d/(\beta V)\right] \quad (1)$$

where I is the emission current, $A = 1.56 \times 10^{-6}$ A V^{-2} eV, $B = 6.83 \times 10^9$ eV$^{-3/2}$ (V m^{-1}), α is the emission area, β is the field enhancement factor, ϕ is the work function, d is the gap between the anode and the point emitter, and V is the applied voltage. The field enhancement factor can be derived from the slope of the F–N plot ($\log(I/V^2)$ vs. $1/V$). Assuming the work function of the CNTs to

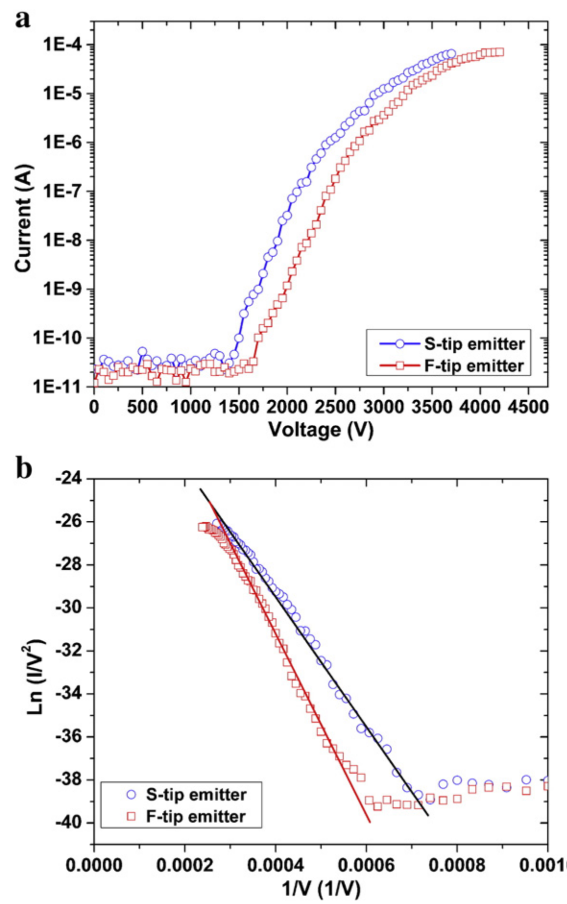

Fig. 4. Field emission characteristics of the two kinds of point emitters. (a) *I–V* curves. (b) The corresponding F–N plots.

be 5.0 eV [21], the field enhancement factors of the F-tip and S-tip emitters can be calculated as 907 and 1264, respectively, which was consistent with the trend in the turn-on voltages.

Field emission stability is one of the most important parameters for the real application of CNT-based field emitters. We applied certain voltage to the emitter, kept for 40 h and monitored the change of the emission current to investigate the field emission stability of both emitters. We applied 4000 V and 3600 V, where the emission current saturated for the F-tip emitter and the S-tip emitter, respectively. Fig. 5 shows the field emission stability of the F-tip and S-tip

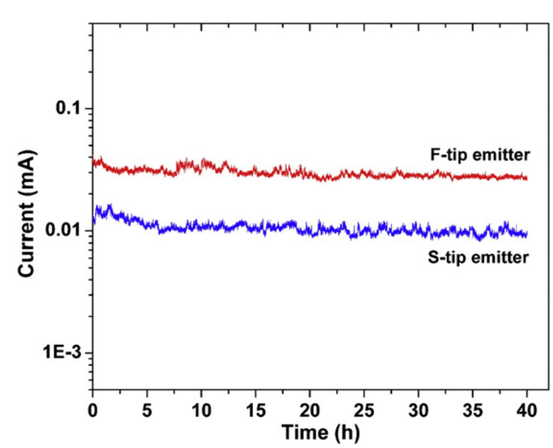

Fig. 5. Field emission stability of the two kinds of point emitters.

Table 1
Field emission properties of various point emitters.

Support	Fabrication method	CNT orientation	Gap	Best emission	Best stability	Reference
W tip	PECVD	Randomly	250 μm	26 μA @ 1200 V	20 h @ 10 μA	[22]
W tip	Inductively coupled plasma-CVD	Randomly	250 μm	51 μA @ 630 V	Over 40 h @ 10 μA	[23]
W tip	Pyrolysis of ferrocene	Randomly	5 cm	1 mA @ 16.5 kV	200 min @ 500 μA	[24]
W wire	Biased thermal CVD	Randomly	1 mm	4 μA @ 6000 V	15 h @ 1.2 μA	[25]
W tip	PECVD	Vertically	1–10 mm	100 μA @ below 10 kV	100 h @ 80 μA	[26]
Pd wire	PECVD	Vertically	0.5 mm	1.3 mA @ 3400 V	Over 500 h @ 1 mA	[27]
Flat W tip	CNT/Ag paste	Randomly	2 mm	465 μA @ 6600 V	40 h @ 100 μA	[28]
Fe needle	CVD	Randomly	20 μm	0.14 μA @ 1040 V	N/A	[29]
Flat Cu tip	PECVD	Vertically	500 μm	70 μA @ 4200 V	40 h @ 40 μA	This work
Sharp Cu tip	PECVD	Vertically	500 μm	65 μA @ 3700 V	40 h @ 13 μA	This work

emitters. Both emitters showed very stable emission current during the stability test. The emission current from the F-tip emitter gradually decreased from an initial current of about 40 μA to around 30 μA. Similarly, the emission current from the S-tip emitter gradually decreased from about 13 μA to 10 μA. There was no sudden degradation of emission current for either of the two kinds of point emitters during the stability test. We attribute the excellent field emission stability of our CNT point emitters to the good morphologies and the strong adhesion between CNTs and the Cu wire.

It is well known that field emission properties are largely dependent on the morphology of the CNTs. Table 1 shows field emission properties of various point emitters on different support materials [22–29]. Most of point emitters were grown on tungsten tip (W tip) and had randomly oriented CNTs [22–25]. To the best of authors' knowledge, this is the first report of the synthesis of VACNTs on Cu wires for the fabrication of point emitters. The CNT point emitters directly grown on Cu wires demonstrated a comparable to or even better field emission properties than other point emitters. Especially, the point emitters on Cu wires showed a very stable field emission current during the stability test for 40 h. This is a good feature for the practical applications of miniaturized X-ray sources and electron beam sources. The different field emission properties were attributed to the morphology difference between the two kinds of CNT point emitters, especially to the density of CNTs. Theoretically, the field enhancement factor $\beta_{Emitter}$ of the emitter can be expressed as a function of the emitter height h and its radius r [30]

$$\beta_{Emitter} = 1.2(2.15 + h/r)^{0.90} \quad (2)$$

As mentioned earlier, for the F-tip emitter, the length of the CNTs is about 1.5 μm and the CNT had a large diameter of 110–140 nm at the tip. For the S-tip emitter, the CNT has a short length in the range of 0.7–1.0 μm and a diameter of around 100 nm. Therefore, we consider that the field enhancement factor of the emitter itself in the F-tip emitter is slightly bigger than or similar to that in the S-tip emitter from Eq. (2). However, the density of CNTs in the S-tip emitter was much lower compared to that in the F-tip emitter. The high density of CNTs can highly degrade the field emission performance of CNT emitters due to the screening effect [19]. Therefore, the S-tip emitter showed a better field emission performance compared with the F-tip emitter. In this work, we consider that the density of CNTs played a dominant role in the field emission because the S-tip emitter demonstrated a better field emission performance than the F-tip emitter. This means that the screening effect which reduces the local electric field is more dominant than the geometry of CNTs in field emission in this work.

4. Conclusions

In summary, vertically aligned CNT point emitters were directly grown on Cu wires with flat or sharp tips. The F-tip emitter showed tapered CNTs with a longer length, a thinner diameter, and a high density whereas the S-tip emitter showed almost cylindrical CNTs with a shorter length, a thicker diameter, and a low density. The CNTs on the F-tip displayed a multi-walled bamboo-liked structure whereas the CNTs on the S-tip showed no clear graphitization due to difficulty in separating a single CNT from the bundles. The two types of point emitters have exhibited excellent field emission performance, such as high emission current at relatively low voltage and longtime emission stability at high current level. The excellent field emission properties are attributed to the point emitter structure and the good contact between the CNTs and the Cu tip. We believe that the CNT point emitters grown on Cu wires are beneficial to the real application of miniaturized X-ray sources and electron beam sources.

Acknowledgements

This work was supported by the National Science Foundation under grant DMR0548061. We are grateful to Dr. Jianyu Huang for his help with the TEM examination of the CNTs.

References

[1] B.Q. Zeng, G.Y. Xiong, S. Chen, W.Z. Wang, D.Z. Wang, Z.F. Ren, Appl. Phys. Lett. 89 (2006) 223119.
[2] X.H. Liang, S.Z. Deng, N.S. Xu, J. Chen, N.Y. Huang, J.C. She, Appl. Phys. Lett. 88 (2006) 111501.
[3] Y. Saito, K. Hamaguchi, K. Hata, K. Uchida, Y. Tasaka, F. Ikazaki, M. Yumura, A. Kasuya, Y. Nishina, Nature 389 (1997) 554.
[4] C.J. Lee, D.W. Kim, T.J. Lee, Y.C. Choi, Y.S. Park, Y.H. Lee, W.B. Choi, N.S. Lee, G.S. Park, J.M. Kim, Chem. Phys. Lett. 312 (1999) 461.
[5] Z.J. Liu, G. Yang, Y.Z. Lee, D. Bordelon, J.P. Lu, O. Zhou, Appl. Phys. Lett. 89 (2006) 103111.
[6] R. Yabushita, K. Hata, J. Vac. Sci. Technol. B 26 (2008) 702.
[7] H.Y. Jung, S.M. Jung, L. Kim, J.S. Suh, Carbon 46 (2008) 969.
[8] G.N. Fursey, Appl. Surf. Sci. 215 (2003) 113.
[9] D. Ferrer, T. Tanii, I. Matsuya, G. Zhong, S. Okamoto, H. Kawarada, T. Shinada, I. Ohdomari, Appl. Phys. Lett. 88 (2006) 033116.
[10] S.I. Jung, J.S. Choi, H.C. Shim, S. Kim, S.H. Jo, C.J. Lee, Appl. Phys. Lett. 89 (2006) 233108.
[11] G. Chen, D.H. Shin, S. Roth, C.J. Lee, Nanotechnology 20 (2009) 315201.
[12] Y. Wei, C.G. Xie, K.A. Dean, B.F. Coll, Appl. Phys. Lett. 79 (2001) 4527.
[13] G. Chen, D.H. Shin, T. Iwasaki, H. Kawarada, C.J. Lee, Nanotechnology 19 (2008) 415703.
[14] Y.Y. Wang, S. Gupta, J.M. Garguilo, Z.J. Liu, L.C. Qin, R.J. Nemanich, Diamond Relat. Mater. 14 (2005) 714.
[15] W.Z. Li, S.S. Xie, L.X. Qian, B.H. Chang, B.S. Zou, W.Y. Zhou, R.A. Zhao, G. Wang, Science 274 (1996) 1701.
[16] K. Hata, D.N. Futaba, K. Mizuno, T. Namai, M. Yumura, S. Iijima, Science 306 (2004) 1362.
[17] Z.F. Ren, Z.P. Huang, J.W. Xu, J.H. Wang, P. Bush, M.P. Siegal, P.N. Provencio, Science 282 (1998) 1105.
[18] D. Mata, M. Amaral, A.J.S. Fernandes, F.J. Oliveira, P. Costa, R.F. Silva, Carbon 49 (2011) 2181.
[19] L. Nilsson, O. Groening, C. Emmenegger, O. Kuettel, E. Schaller, L. Schlapbach, H. Kind, J.M. Bonard, K. Kern, Appl. Phys. Lett. 76 (2000) 2071.
[20] R.T.K. Baker, Carbon 27 (1989) 315.
[21] N. de Jonge, M. Allioux, M. Doytcheva, M. Kaiser, K.B.K. Teo, R.G. Lacerda, W.I. Milne, Appl. Phys. Lett. 85 (2004) 1607.
[22] S.H. Heo, A. Ihsan, S.O. Cho, Appl. Phys. Lett. 90 (2007) 183109.

[23] J.P. Kim, Y.K. Kim, C.K. Park, H.Y. Choi, C.H. Shon, J.U. Kim, J.S. Park, Diamond Relat. Mater. 18 (2009) 486.
[24] R.B. Sharma, V.N. Tondare, D.S. Joag, A. Govindaraj, C.N.R. Rao, Chem. Phys. Lett. 344 (2001) 283.
[25] Y.B. Zhang, S.P. Lau, L. Huang, M. Tanemura, Appl. Phys. Lett. 86 (2005) 123115.
[26] Y. Sakai, D. Tone, S. Nagatsu, T. Endo, S. Kita, F. Okuyama, Appl. Phys. Lett. 95 (2009) 073104.
[27] S. Kita, Y. Sakai, T. Fukushima, Y. Mizuta, A. Ogawa, S. Senda, F. Okuyama, Appl. Phys. Lett. 85 (2004) 4478.
[28] S.H. Heo, A. Ihsan, S.H. Yoo, G. Ali, S.O. Cho, Nanoscale Res. Lett. 5 (2010) 720.
[29] H.F. Cheng, Y.M. Tsau, T.Y. Chang, T.S. Lai, T.F. Kuo, I.N. Lin, Physica B 323 (2002) 158.
[30] C.J. Edgcombe, U. Valdrè, Philos. Mag. B 82 (2002) 987.